NUCL SCI TECH (2019) 30:17
https://doi.org/10.1007/s41365-018-0538-2

CrossMark

Integrity control of an RBMK-1500 fuel rod locally oxidized under a bounding reactivity-initiated accident

Hamid Boucherit[1] · **Algirdas Kaliatka**[2] · **Azzedine Lounis**[3]

Received: 1 July 2017 / Revised: 8 April 2018 / Accepted: 9 June 2018 / Published online: 2 January 2019

Abstract In 2007, the license for the second reactor unit of the Ignalina nuclear power plant was renewed considering the safety-related modifications introduced in this reactor. The Safety Analysis Report for this reactor unit was prepared with more strict criteria. The bounding reactivity-initiated accident (RIA) performed by the Lithuanian Energy Institute could be mentioned as an example. The performed analysis demonstrated that even when the worst initial conditions and possible uncertainties are considered, the fuel cladding remains intact. However, the analysis was performed assuming a fresh fuel assembly. In this study, an analysis of the fuel rod cladding behavior in the RBMK-1500 reactor following a bounding RIA is performed using the computational codes FEMAXI-6 and RELAP5. The analysis is extended by modeling an oxide layer (nodular corrosion) on the external surface cladding. An uncertainty and sensitivity analysis was performed using a method developed by the Society for Plant and Reactor Safety, employing the Software for Uncertainty and Sensitivity Analyses, in order to evaluate the effect of the oxide layer on the inside and outside fuel rod temperatures. The results of the thermo-mechanical analysis (stress, strain, and enthalpy) for a local oxide layer with a thickness of 70 µm show that despite the exceeded limit of allowed linear power density, the fuel rod is under acceptable safety conditions.

Keywords Safety · Reactivity-initiated accident · Corrosion · RBMK-1500 · FEMAXI-6 · RELAP5 · Software for Uncertainty and Sensitivity Analyses (SUSA)

1 Introduction

RBMK reactors are graphite-moderated channel-type generation-II reactors. They are one of the oldest commercial reactor designs, still widely used. A total of 11 RBMK-1000 reactors operating in Russia have been retrofitted with various safety updates.

The Lithuanian Ignalina RBMK-1500 reactors differ from the RBMK-1000 reactors commissioned in Russia and Ukraine in the significantly increased electrical power (1500 MW against 1000 MW). After the Chernobyl disaster, the electric power was decreased down to 1360 MW. (The thermal power capacity was decreased from 4800 MW to 4200 MW.) The RBMK-1000 and RBMK-1500 reactors belong to the boiling-water-cooled type of reactors, whose pressure of the steam–water mixture in the core outlet is approximately 7.0 MPa. Both RBMK-1500 units in Lithuania (Ignalina Nuclear Power Plant (NPP)) were shutdown for decommissioning in 2004 and 2009.

The nuclear fuel in the RBMK-1500 is a low-enriched uranium, loaded into fuel rods with a diameter of 13.6 mm with cladding, made from a zirconium–niobium alloy. The initial fuel enrichment was 2%; since 1997, the loaded fuel enrichment is 2.4%. Fuel assemblies are made of 18 rods; each of them is positioned in an individual vertical fuel channel. There are 1661 vertical fuel channels with an

✉ Hamid Boucherit
h-boucherit@crnd.dz; hboucherit@yahoo.fr

1 Division of Fuel Technology, Nuclear Research Center of Draria, 16050 Algiers, Algeria

2 Lithuanian Energy Institute, 44403 Kaunas, Lithuania

3 Science and Materials Engineering Laboratory, University of Sciences and Technology Houari Boumediene, 16042 Algiers, Algeria

active fuel length of 7 m. The fuel burnup is 21.6 MWd/kg, in accordance with safety-imposed restrictions related to minimization of the steam reactivity coefficient. The fuel assemblies are cooled by water, which enters at the bottom at a subcooling temperature of 30 °C and exits the channels at an average steam volume fraction of approximately 76%. The coolant flow rate at the design power is approximately 4–6 kg/s through each fuel channel. The important components, such as the fuel channel and fuel cladding, of the RBMK-1500 reactor type, such as the boiling water reactor (BWR), are made of zircaloy. The fuel cladding, utilized in an oxygenated reactor coolant, is subject to accelerated oxidation promoted by synergistic effects of dissolved oxygen and radiation.

The zircaloy cladding and structures may undergo a process of corrosion according to the following reaction: $Zr + 2H_2O \rightarrow ZrO_2 + 4H$. The corrosion leads to oxidization of the surface in contact with the primary circuit water by hydriding the underlying metal. It is important to follow the evolution of corrosion in the reactor. It is well known that corrosion significantly affects thermo-mechanical properties of zircaloy cladding material [1]. This oxidation is a highly exothermic reaction. However, in this case, when the oxidation process is very slow, an additional heat is insignificant. The accelerated oxidation has two components: One of them is uniform, while the other one is nodular. The formation of nodules may lead to: (i) a locally reduced thickness of the fuel rod cladding, (ii) local increase in the temperature of the cladding, (iii) increase in the quantity of corrosion products, and affect (iv) the refrigerant, (v) mechanical interaction between fuel elements, and (vi) supporting grid.

In a previous study, Pabarcius et al. [2] simulated a bounding reactivity-initiated accident (RIA) for a fresh fuel in the Ignalina NPP reactor in order to evaluate the fuel cladding integrity. They performed a bounding analysis, as a computational analysis of all possible RIAs may not be practicable. Therefore, one limiting case was selected, which was referred to as bounding or enveloping scenario. This scenario has been chosen according to the International Atomic Energy Agency (IAEA) methodology [3], such that it presents the largest possible challenge to relevant acceptance criteria and limits the performance parameters of safety-related equipment.

However, it has been revealed that the fuel rod is always under acceptable safety conditions even though the linear power was beyond the allowed limits. Unlike the analysis performed in Ref. [2], in this study, we consider the presence of corrosion products on the outside surface of fuel rods, located at a position where the power peak reaches the highest rate owing to the RIA. The effects of changes in thermo-mechanical properties are discussed. In addition, uncertainty and sensitivity studies were performed using the Society for Plant and Reactor Safety (GRS) method in order to analyze the effects of geometrical, thermal conductivity model, and oxide layer uncertainties on the temperatures of the fuel and cladding. The effect of hydride is not considered in this study.

For the fuel behavior analysis, we use three computer codes: QUABOX–CUBBOX, FEMAXI-6, and RELAP5. The QUABOX–CUBBOX code, developed by GRS (Germany) [4], provides a detailed analysis of the reactor core behavior based on three-dimensional (3D) neutronic models. These models solve two-energy-group neutron diffusion equations, including reactivity feedback effects caused by changes in coolant flow conditions and changes in the fuel rod temperature. The solution is based on a flux expansion method using local polynomials, which enables to calculate one-dimensional (1D), two-dimensional (2D), and 3D core configurations. Since 1990, the code was adapted to the features of RBMK-1000 reactors, while since 1995, it was additionally adapted to consider special requirements of RBMK-1500 reactors. The code was used for audit calculations during the review of the Ignalina NPP Safety Analysis Report (SAR) for Unit 1 and for preparation of the SAR for Unit 2. Later, the Q/C-H code was applied for an independent assessment of the shutdown system modification at Unit 2. In this study, the QUABOX–CUBBOX code is used for a calculation of the linear power for a selected fuel rod in the RBMK-1500 core in the case of a bounding RIA.

The FEMAXI-6 code, developed by the Japan Atomic Energy Agency (JAEA), is designed to predict thermal and mechanical behaviors of a light water reactor fuel rod during normal and transient (not accident) conditions. It can also analyze the integral behavior of the whole fuel rod throughout its life as well as the localized behavior of a small part of the fuel rod. The temperature distribution, radial and axial deformations, fission gas release, and inner gas pressure are calculated as a function of the irradiation time and axial position. The stresses and strains in the pellet and cladding are calculated, and a pellet–cladding mechanical interaction (PCMI) analysis is performed. In addition, the thermal conductivity degradation of the pellet and cladding waterside oxidation could be modeled [5]. In this study, the FEMAXI-6 code is used for the analysis of thermal and mechanical behaviors of the selected fuel rod.

The RELAP5 code [6] has been developed by the USA Idaho National Engineering Laboratory (INEL) for a best-estimate transient simulation of light water reactor coolant systems during postulated accidents. This code models the coupled behavior of the reactor coolant system and core for loss-of-coolant accidents (LOCA), and operational transients, such as an anticipated transient without scram, loss of offsite power, loss of feed water, and loss of flow. In this study, the RELAP5 code is used in order to calculate the fuel pellet and cladding temperatures, thermal–hydraulic parameters in the core, and critical heat flux for fuel rods during the analyzed RIA.

2 Analysis of a bounding RIA for RBMK-1500

In 2007, the license for the second reactor unit of the Ignalina NPP was renewed considering the safety-related modifications introduced in this reactor. The SAR for the second reactor unit was prepared considering more strict criteria. The most typical example is the analysis of RIAs. In addition to the detailed investigation of different RIAs and analysis of the bounding case, the evaluation of possible uncertainties was performed upon the request of the Lithuanian Nuclear Regulatory Authority. An accident related to spurious withdrawal of a single control rod in the central part of the core at the maximum permissible thermal reactor power (4200 MW) was selected for a more detailed investigation. This event leads to a more significant change in core parameters; therefore, it was denoted as "bounding RIA".

Typically, RIAs for plants with RBMK-type reactors are classified as design basis accident (DBA), with the following safety criteria [7]:

- Maximum fuel pellet temperature ≤ 2800 °C,
- Volume-average fuel enthalpy ≤ 710 kJ/kg,
- Maximum cladding temperature ≤ 700 °C,
- Maximum local cladding oxidation ≤ 18%.

However, assessing the real probability of these events, such type of incidents should be considered more strictly. It was also decided to evaluate the acceptance criteria for the following anticipated transients:

- Fuel linear power ≤ 485 W/cm.
- Calculated critical heat flux margin coefficient from the fuel assembly to the coolant ≥ 1.

The modeling of such a bounding RIA in an RBMK-1500 was performed in the Lithuanian Energy Institute (LEI) [2, 8]. However, the RIA was simulated for a fresh fuel in order to evaluate the fuel cladding integrity. In this study, we simulate nodular corrosion located at the height of the fuel rod, corresponding to the power peak and attributed to the RIA.

For the process modeling in the RBMK-1500 reactor core and analyses of RIAs, the QUABOX/CUBBOX-HYCA (Q/C-H) code was used in the LEI for the case of erroneous withdrawal of one manual control rod in the central part of the reactor core at the nominal power. The change in the fuel rod power in the fuel channel with an initial high power (3.75 MW) is presented in Fig. 1.

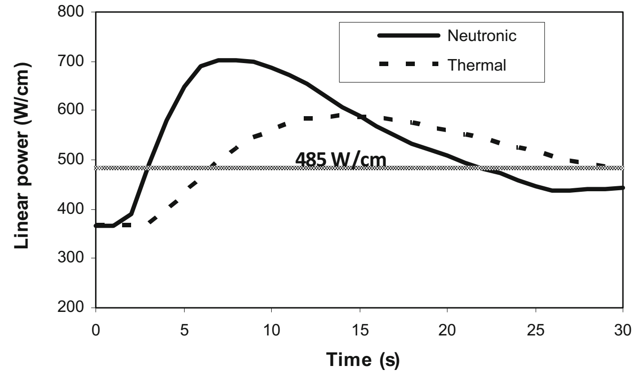

Fig. 1 Maximum power in the fuel rod during a bounding RIA simulation [2]

In our analysis, we assumed that the power peak in Fig. 1 occurs after an irradiation basis that lasts approximately 312 days with an average linear power of 250 W/cm. This power peak is located at a height of 107 cm from the bottom of the fuel rod for a maximum linear neutronic power of 714 W/cm. The "neutronic" power is the power generated inside the fuel pellets. The so-called thermal power, i.e., the power transferred from the fuel rod cladding to the coolant, is used for the safety evaluation. The simulation of the RIA showed that the peak thermal power is equal to 589 W/cm, higher than the limit of the acceptance criterion (485 W/cm). A gap closure between the pellets and cladding in some segments appeared for a short period of time (5–20 s) after the beginning of the incident, due to swelling generated by high amount of heat and radial displacements of fuel pellets.

3 Corrosion modeling

Nodular corrosion occurs in certain cases in the form of scattered buttons very close to each other (Fig. 2). The nodular corrosion could propagate along a distance of several centimeters. For simplicity, we consider that the

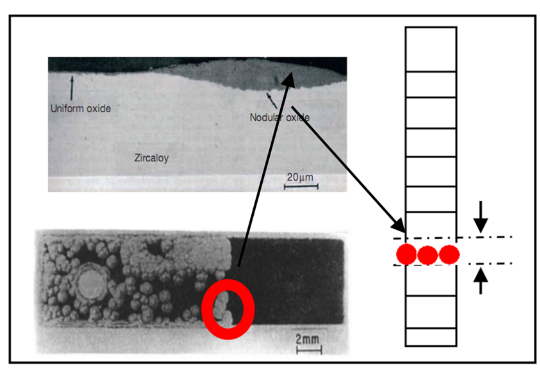

Fig. 2 Typical appearance of nodular corrosion in visual inspection and metallographic investigation [1]

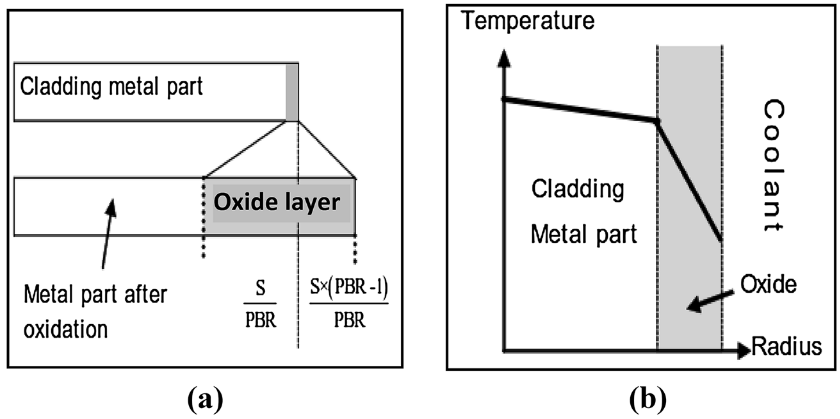

Fig. 3 **a** Volume increase and **b** temperature distribution inside the cladding owing to the oxide layer [5]

nodular corrosion has the form of a homogeneous ring around the cladding external surface, as shown in Fig. 2.

A decrease in the thickness of the cladding metal part and an increase in the cladding outer diameter (see Fig. 3) can be expressed as *S/PBR* and *S*(*PBR-1*)*/PBR*, respectively [5],where *S* is the oxide layer thickness and *PBR* is the Pilling–Bedworth ratio. A *PBR* value of 1.56 was used. However, considering the Applied Energy Group data [9], in our calculation, with slight pessimism, we considered nodular corrosion with a thickness of 70 µm. It is worth noting that the effect of hydride was not considered in this study.

4 Modeling of a fuel rod locally oxidized under the bounding RIA with FEMAXI-6 and RELAP5

The models of a locally oxidized RBMK-1500 fuel rod obtained using RELAP5 and FEMAXI-6 are presented in Fig. 4a, b, respectively. The fuel rod is divided into 12 segments along the height. The pellet in the radial direction is discretized into ten rings, while the cladding into four rings [two in the base metal (defined below as elements 11 and 12) and two in the corrosion layer (defined below as elements 13 and 14)]. The oxide layer is considered to be spread out over the segment 4 where the peak power is generated (1.07 m from the bottom of the core).

The thermo-hydraulic parameters were calculated by RELAP5 to compare the results with those of FEMAXI-6. In the RELAP5 calculations, the pellets and cladding are modeled using RELAP5 "heat structure" elements (used for modeling of heat transfer) to evaluate thermal properties (density, thermal conductivity, and volumetric heat capacity) of the pellet and cladding materials. The gap between the pellets and cladding in the fuel rod is modeled by an additional material structure layer with the specific thermal conductivity of the gasses inside the fuel rod. Owing to swelling of the pellets, the gap between the pellets and cladding disappears, and the surface of the pellets touches the surface of the cladding. This leads to a better heat transfer from the pellet to the coolant through the cladding. In order to model such a situation in the RELAP5 calculation, the value of the thermal conductivity of the structure representing the gap was increased to

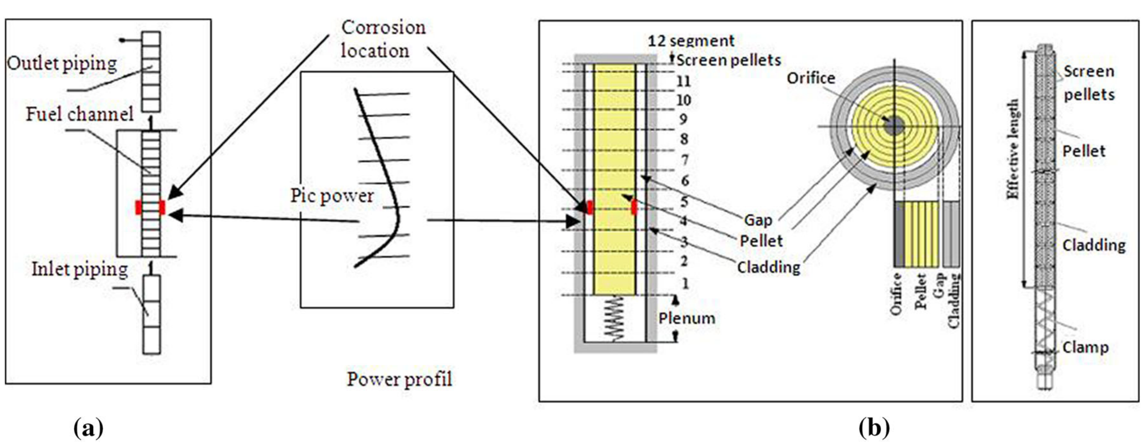

Fig. 4 Modeling of a locally oxidized fuel rod by: **a** RELAP5 and **b** FEMAXI-6 [10]

simulate the enhanced heat transfer during the gap closure within the time interval of 5–20 s.

5 Results and interpretations

5.1 Thermal analysis

Using FEMAXI-6, the temperatures profile evolutions in the pellet (parabolic shape) and cladding (linear shape) during the power increase for the 70-µm-thick cladding oxide are shown in Fig. 5. The FEMAXI-6 code was used to calculate the pellet central temperature in the presence of a central hole with a size of 2 mm. During the bounding RIA, the fuel pellet temperatures, cladding temperatures, and heat flux evolutions are calculated using the FEMAXI-6 and RELAP5 codes, as shown in Figs. 6, 7 and 8, respectively. These results are obtained for the segment at a height of 1.07 m from the fuel assembly bottom where gap closure is assumed within the time interval of 5–20 s.

Figure 6 reveals that the simulated oxide layer (70 µm) compared to the fresh fuel rod (0.1 µm) leads to increases in the pellet and cladding temperatures of approximately 100 °C. The central pellet temperature with the corrosion layer calculated using the FEMAXI-6 code is approximately 2500 °C (Fig. 6a), whereas that obtained using RELAP5 is approximately 2100 °C (Fig. 6b).

As shown in Fig. 7, the radial temperature gradients in the cladding obtained by FEMAXI-6 and RELAP5 are approximately 100 °C and 70–120 °C, respectively. Therefore, the highest calculated pellet temperature is lower than that of the safety criteria for the UO_2 fuel pellet (2840 ± 50 °C) [11]. Similarly, the temperature in the cladding significantly differs from 700 °C, which represents a temperature limit where plastic deformation of the cladding may appear [7]. During the bounding RIA, the

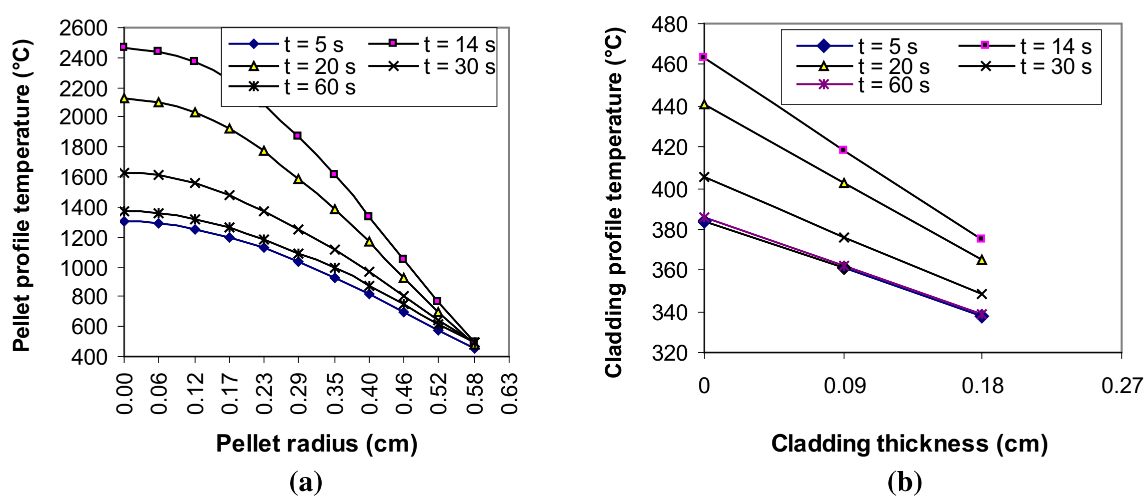

Fig. 5 FEMAXI-6 profile temperatures in the: **a** pellet and **b** cladding

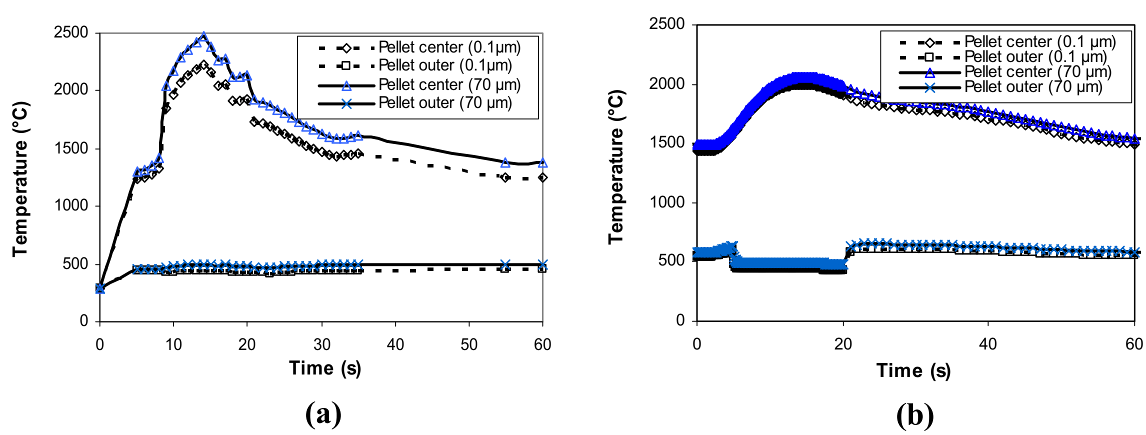

Fig. 6 Temperatures in the fuel pellet calculated by: **a** FEMAXI-6 and **b** RELAP5

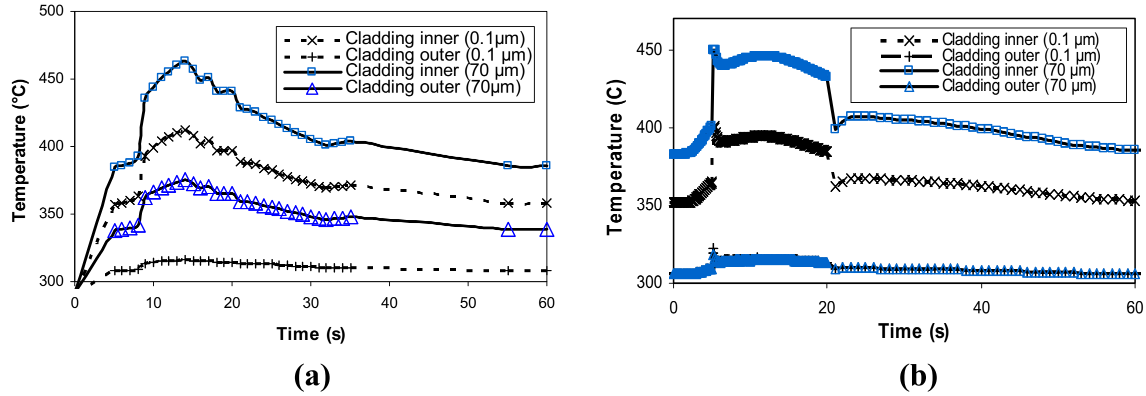

Fig. 7 Temperatures in the cladding calculated by: **a** FEMAXI-6 and **b** RELAP5

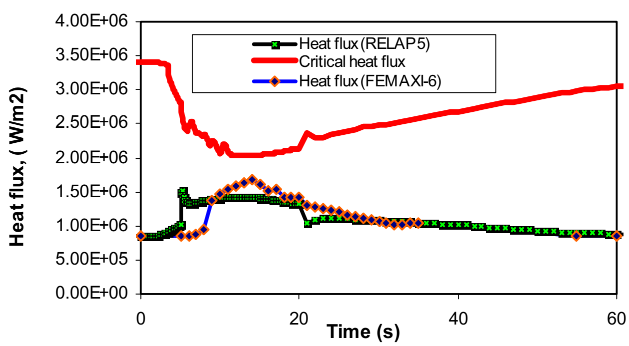

Fig. 8 Real heat fluxes (RELAP5 and FEMAXI-6) compared to the critical heat flux

cladding oxidation layer thickness increases by approximately 1.5 µm. This value is below the limited design threshold of 17–18% of the cladding thickness before occurrence of an embrittlement risk [3, 12].

In order to verify the type of flow regime (dependent on the cooling conditions and heat flow in the fuel channel) during the power peak, we have to ensure that this regime has not reached the critical limit.

As shown in Fig. 8, the heat fluxes deduced from the FEMAXI-6 and RELAP5 codes for the investigated segment are below the critical heat flux; therefore, the dry-out is not reached.

The increase in the average enthalpy volume of the fuel pellet is calculated from the highest temperatures obtained by FEMAXI-6 (the worst case), rather than from the lowest temperatures obtained by RELAP5. The fuel temperature and corresponding enthalpy results are reported in Table 1. After the power peak, the increase in the enthalpy value reached 500 kJ/kg, which is below the acceptance limit of 710 kJ/kg.

According to the previous results, the calculated values using FEMAXI-6 are comparable to those using RELAP5. Both codes show that the fuel rod, from a thermal point of view, is below the threshold safety limits in the case of a bounding RIA. However, the simulation using RELAP5 of the corrosion layer and gap closure between the pellets and cladding is not very reliable in the case of the bounding RIA. Therefore, the FEMAXI-6 code is used for the mechanical calculation.

5.2 Mechanical parameter calculation with FEMAXI-6

Stress and strain analyses are performed using the finite-element method with quadrangular elements with four degrees of freedom, as presented in Fig. 9.

The pellet–cladding gap evolution as a function of the fuel rod height for the maximum value of the power peak during the bounding RIA ($t \approx 15$ s) is shown in Fig. 10, which reveals that there is no significant difference between the fresh fuel (0.1-µm-thick ZrO_2 layer) and case of localized corrosion (70 µm). The pellet–cladding contact in this incident was established over a length exceeding half of the height of the fuel rod. The contact force is slightly higher (by approximately 5 MPa) in the case of the localized corrosion, compared to that for the fresh fuel. This may be a source of circumferential constraints in the cladding, which induces exfoliation due to nodular corrosion.

Furthermore, during the analyzed incident, the burnup is still constant, but the central fuel pellet temperature increases beyond the limit curve of Vitanza [13, 14] (Fig. 11); this leads to an accelerated fission gas release of 0.5% to 0.52% (Fig. 12). The FEMAXI-6 code cannot model a significant release of fission gas from the pellet in the case of a fast power increase. However, RIAs in the RBMK reactor are slow; the power in the reactor core increases within few seconds, as the RBMK is a channel-type reactor, and, owing to the presence of graphite around each fuel channel and large distance between fuel assemblies, the neutron reaction time is comparatively long. The suitability of the FEMAXI-6 code for the analysis of slow

Table 1 Fuel enthalpy evaluation

Time moment	Maximum average temperature of the fuel pellet		Volume-averaged specific enthalpy of the fuel pellet (UO_2)	Enthalpy increase
0 s	1306.1 °C	1579.1 K	400 kJ/kg	(900–400) kJ/kg = 500 kJ/kg
15 s	2467.8 °C	2740.8 K	900 kJ/kg	

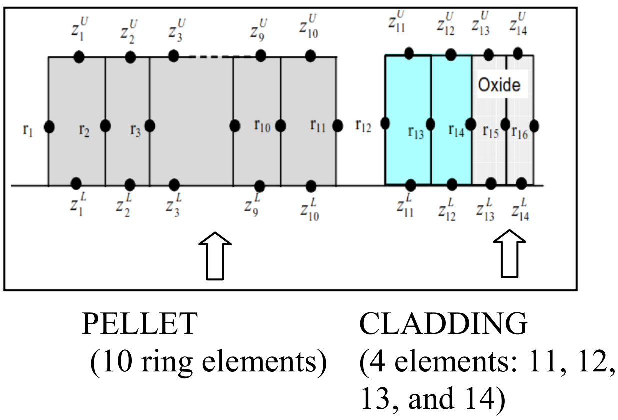

Fig. 9 Mesh division of the finite-element method (for one axial segment)

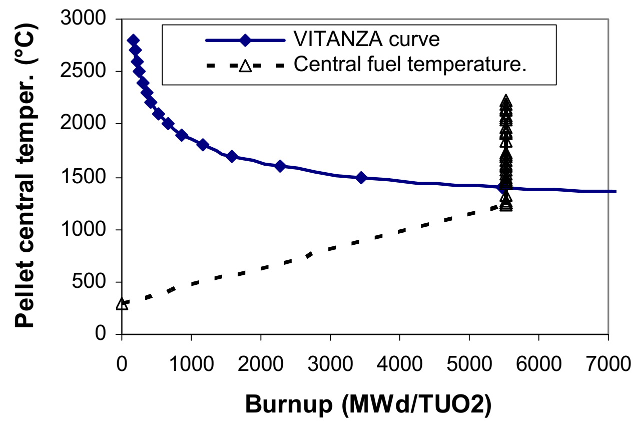

Fig. 11 Central pellet temperature during the bounding RIA and Vitanza curve

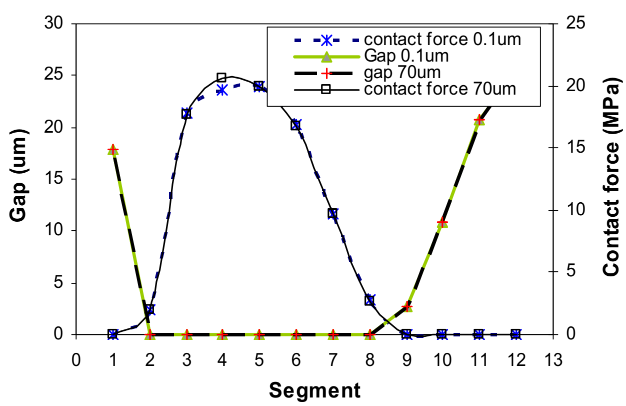

Fig. 10 Gap and contact force during the RIA

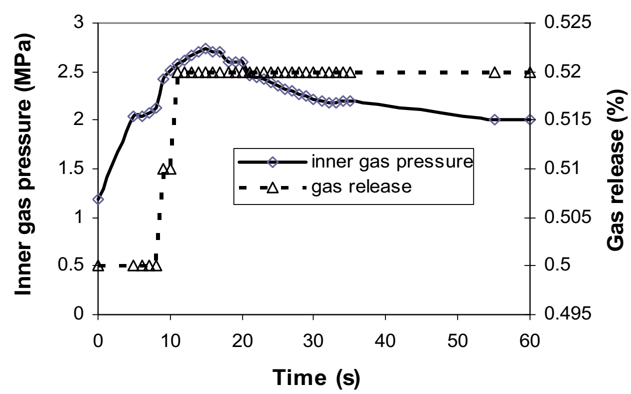

Fig. 12 Gas release and pressure in the fuel rod during the bounding RIA

RIAs was confirmed by the code developers. This explains the result that the fission gas release in the presented analysis has a negligible effect (see Fig. 12).

The released gas from the fuel pellets slightly increases the pressure inside the fuel rod. Outward creep does not occur, as the internal pressure of the rod is still smaller than the nominal pressure in the reactor cooling system during normal operation (7 MPa). However, it is important to verify whether the cladding values under the bounding RIA are below the stress and strain safety limits.

5.3 Strain in the cladding (segment 4: peak power)

The cladding strain analysis for the peak power in segment 4 presented in Fig. 13 shows a sensitive hoop strain increase, compared to the radial and axial strains. The variation of 0.2% of the hoop strain remains below the threshold tolerated by the design (maximum hoop elastic and plastic strains of 1% and maximum permanent axial and tangential strains of 2.5%) owing to the fuel swelling at the end of the fuel life [15].

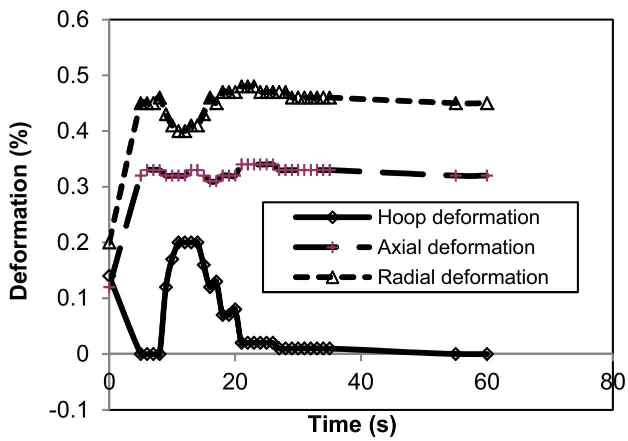

Fig. 13 Strains in the cladding during the bounding RIA

5.4 Stress in the cladding (segment 4: peak power)

The hoop and axial stresses inside the cladding at the peak power level are shown in Figs. 14 and 15, respectively. Figure 14b shows a hoop stress jump between elements 12 and 13 in segment 4. This increase in the hoop stress is mainly due to the different material properties (such as the Young's modulus, thermal conductivity, and thermal expansion) leading to different responses of the base metal and oxide at the interface. Figure 14b shows that the hoop stresses for the 70-µm-thick oxide layer and fresh fuel are similar.

As shown in Fig. 15, despite the power peak and the presence of the oxide layer in segment 4, the maximum axial stress is observed in the upper extremity of the fuel rod, owing to the axial gradient temperature in the cladding; the increase in the cladding temperature allows the cladding to dilate and adapt to the stress. It is worth noting that the maximum calculated stress in the cladding is well below the yield stress of zirconium (250–310 MPa); generally, conservative design limits are used for the stress (yield or tensile strength) of approximately 1% at the operating temperature [13].

In order to evaluate the effect of the oxide layer on the hoop stress evolution, calculations were done for different layer thicknesses (from 0 to 90 µm). The reported results in

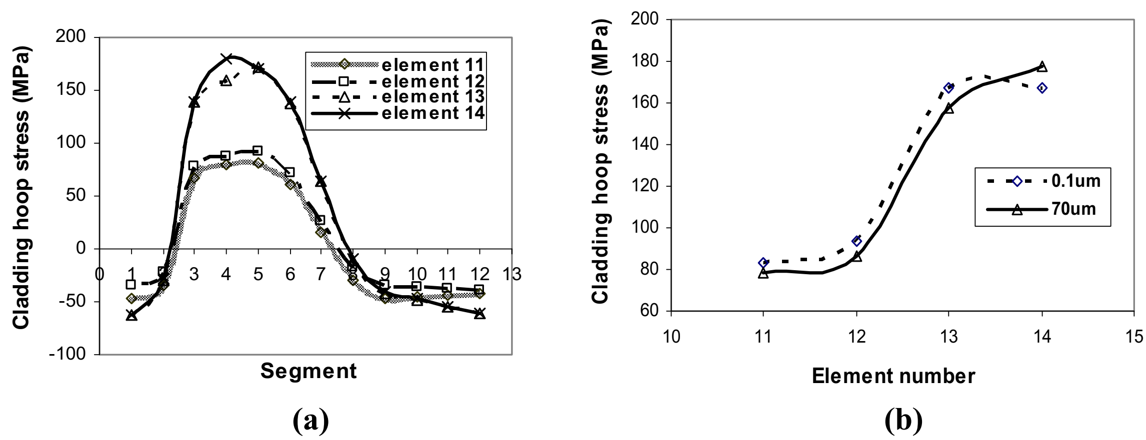

Fig. 14 Cladding hoop stress (70-µm-thick oxide layer): **a** along the fuel rod and **b** at the peak power (segment 4)

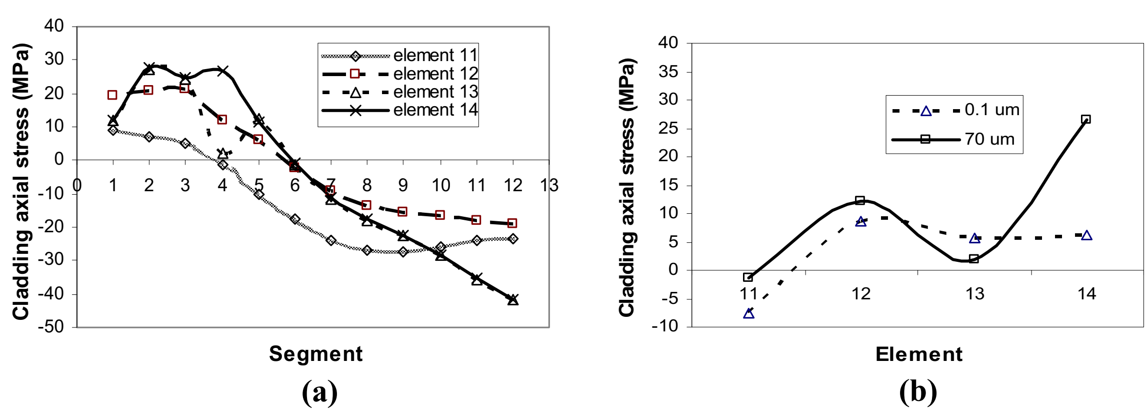

Fig. 15 Cladding axial stress (70-µm-thick oxide layer): **a** along the fuel rod and **b** at the peak power (segment 4)

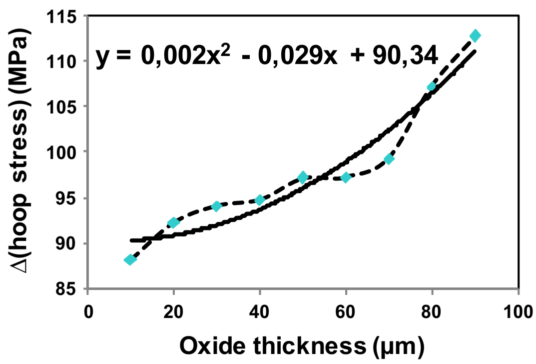

Fig. 16 Hoop stress gradient as a function of the oxide layer thickness

Table 2 Uncertainties of parameters

Parameter name	Distribution type	Distribution values		Unit
CDIN	Normal	$\mu = 1.175$	$\sigma = 0.0025$	cm
CDOUT	Normal	$\mu = 1.354$	$\sigma = 0.0045$	cm
PDIA	Normal	$\mu = 1.148$	$\sigma = 0.002$	cm
OXTH	Uniform	Min = 63	Max = 77	μm
FPTH	Uniform	Min = 0.9	Max = 1.09	

μ average value, σ standard deviation

Fig. 16 show a parabolic evolution of the Δ(hoop stress) as a function of the oxide layer thickness.

6 Uncertainty and sensitivity analysis

Uncertainty and sensitivity analyses were performed using the GRS approach [16], employing the Software for Uncertainty and Sensitivity Analyses (SUSA) [17]. The GRS approach is based on a systematic identification of relevant physical processes and probabilistic quantification of the uncertainties of corresponding parameters. The selection of parameter values according to their specified probability distributions, their combination, and evaluation of calculation results in the GRS method is performed using a statistical technique. Random uncertain parameter values of vectors are generated by the Monte Carlo method. In each code calculation, all uncertain parameters are simultaneously varied. The number of code calculations depends on the requested probability content and confidence level of statistical tolerance limits used in the uncertainty statements of the results. The required minimum number n of calculation runs is obtained by the Wilks' formula. In our case, we use the one-sided statistical tolerance limit. Therefore, for a confidence of 95% and probability of 95%, only 59 calculations (runs) should be done.

The effects of the uncertainties of five parameters on the values of the central fuel pellet temperature and cladding external temperature were evaluated. The parameters (see Table 2) are selected among those that can affect the heat transfer from the fuel pellet to the coolant. They are: oxide layer thickness (OXTH), fuel pellet diameter (PDIA), pellet thermal conductivity (magnification factor, FPTH), and inside and outside cladding diameters (CDIN and CDOUT, respectively). The ranges of the uncertainties and distribution functions for the geometrical parameters were assumed from NUREG/CR-700 [18]. The parameter OXTH and factor FPTH with uniform distributions simulate 10% [19] and 20% [20] of the parameters' uncertainties (see Table 2), respectively.

The calculations using a random sampling of parameters (Table 2) provide a range of internal and external fuel temperature values shown in Fig. 17. The variation is approximately 400 °C for the central fuel pellet temperature and 20 °C for the outside temperature of the cladding.

Sensitivity measures indicate the influence of uncertainty in the input parameters on the calculation results. In our case, the Spearman rank correlation coefficient (SRCC), which varies from − 1 to + 1, is used as a sensitivity measure (particularly for nonlinear models). In Fig. 18, the magnitudes of the bars indicate the sensitivities

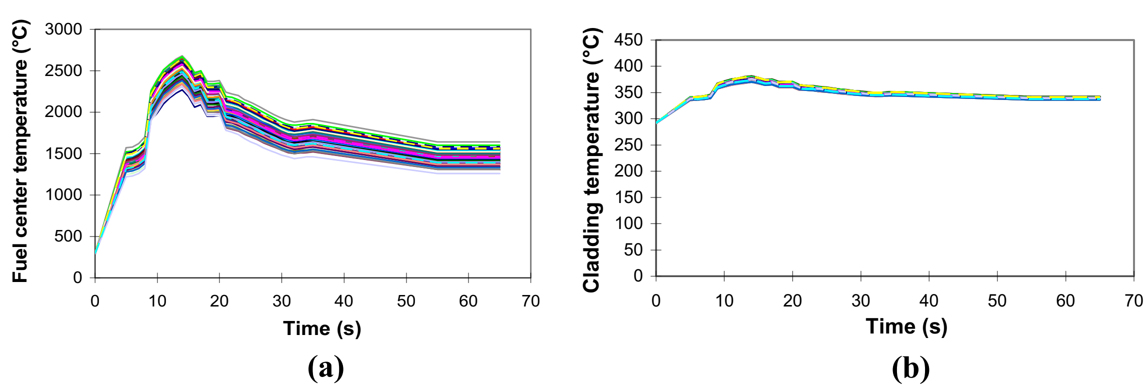

Fig. 17 Temperatures from uncertainties (59 runs) in the: **a** center of the pellet and **b** external face cladding

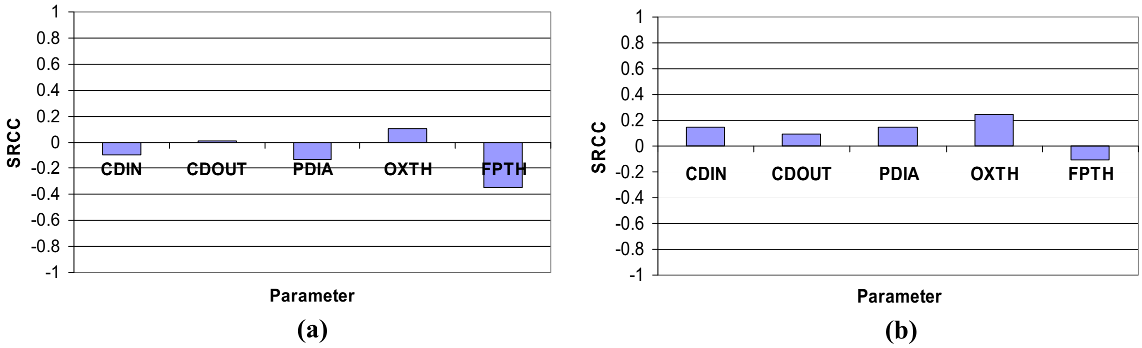

Fig. 18 Sensitivities for the different input variables for the temperatures in the: **a** center of the pellet and **b** external face cladding

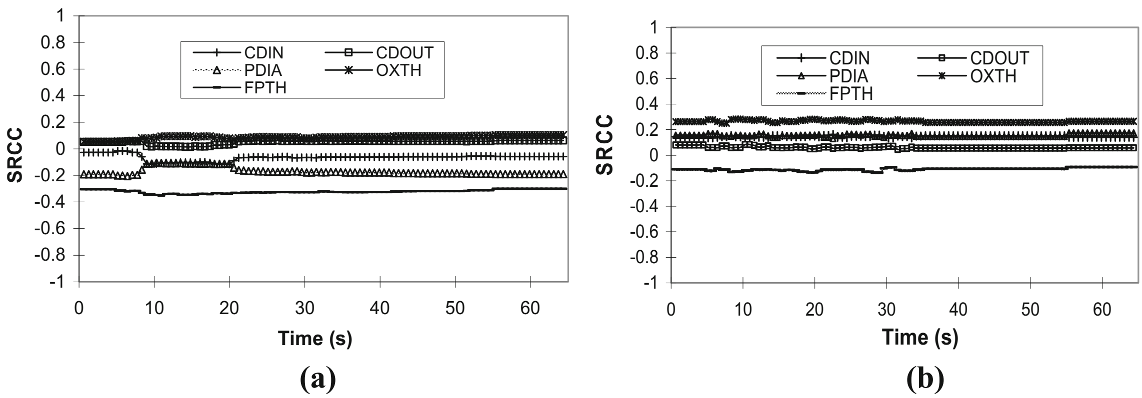

Fig. 19 SRCC for the different input variables for the temperatures in the: **a** center of the pellet and **b** external face cladding

of the corresponding input parameters to the calculated central fuel temperature and external cladding temperature during the power peak phase. Positive sign implies that the input parameter value and result tend to shift in the same direction, while negative sign implies that the input parameter value and result tend to shift in opposite directions. The sensitivities of the input parameters on the central fuel temperature and external cladding temperature as a function of the time during the power peak are presented in Fig. 19.

Figures 18a and 19a show that the FPTH parameter has the highest influence on the central pellet temperature results. This parameter has negative influence on the results, i.e., its increase leads to a lower temperature in the fuel center; however, during the power peak, its deviation is negligible. The parameters CDIN and PDIA have negative influences, while the parameter OXTH has positive influence; these parameters only slightly influence the results. For the external face cladding temperature calculation results, OXTH has the highest influence (see Figs. 18b and 19b). This parameter has positive influence on the results, i.e., its increase leads to a higher temperature in the external cladding. The variations in the parameters CDIN, CDOUT, and PDIA (negative influences) and parameter OXTH (positive influence) have insignificant influences on the results.

7 Conclusion

We analyzed the fuel rod behavior in an RBMK-1500 reactor in the case of an RIA at the most conservative initial and boundary conditions (“bounding” case). During the bounding RIA in the RBMK-1500 (spurious withdrawal of a single control rod in the central part of the core), the linear power criterion for fuel rods was exceeded; therefore, a detailed analysis to investigate the behavior of the fuel rods was required. Unlike previously performed analyses, in this study, the bounding RIA was modeled considering the maximum possible layer thickness of nodular corrosion on the outside surface of the fuel rod after one year of reactor’s normal operation. Fuel rod models were developed using the FEMAXI-6 and RELAP5 codes in order to simulate the nodular corrosion.

The results of the performed sensitivity analysis showed that the oxide layer thickness was the most important parameter affecting the cladding temperature. This result confirmed our decision to analyze the influence of the corrosion (oxide) layer on the behavior of the fuel rod cladding. The calculations done using the FEMAXI-6 and RELAP5 codes on the behavior of the fuel pellets and cladding during the bounding RIA revealed reasonable agreement between their results. The calculated fuel pellet and cladding temperatures under evaluation of possible uncertainties at probability content of 95% and confidence level of 95% are below the acceptance limits. On the other hand, the increase in the fuel enthalpy due to the RIA was below the criterion related to fuel damage. The calculated values of the stress in the pellets and calculated stress and strain in the cladding are below the levels of thresholds tolerated by the design.

All of the results of the performed detailed analyses showed that even when the fuel linear power criterion is exceeded, the cladding of the affected fuel rod remains intact despite the pellet–cladding interaction.

References

1. T.R. Allen, R.J.M. Konings, A.T. Motta, Corrosion of zirconium alloys. Comp. Nucl. Mater. **5**, 49–68 (2012)
2. R. Pabarcius, A. Kaliatka, A. Marao, Analysis of fuel rod behaviour during limiting RIA in RBMK plants. J. Kerntechnik **75**, 329–336 (2010)
3. IAEA, Deterministic Safety Analysis for Nuclear Power Plants. Specific Safety Guide No. SSG-2 (Vienna, 2009)
4. QUABOX-CUBBOX software, https://www.grs.de/en/simulation-codes/quabox-cubbox
5. M. Suzuki, H. Saitou, Light Water Reactor Fuel Analysis Code FEMAXI-6 (Ver.1), detailed structure and user's Manual. JAEA-Data/Code 2005-003 (2006)
6. C.D. Fletcher, R.R. Schult, RELAP5/MOD3 Code Manual, User's Guidelines, NUREG/CR-5535, INEL-95/0174, Vol. 5, Rev. 1 (1995)
7. IAEA, Accident analysis for nuclear power plants with graphite moderated boiling water RBMK reactors. Safety Reports Series No. 43 (Vienna, 2005)
8. R. Pabarčius, A. Tonkūnas, Definition of conservative conditions for RIA analysis in the modernized RBMK reactor core. J. Kerntechnik **75**, 178–184 (2010)
9. L. Lunde, Special features of external corrosion of fuel cladding in boiling water reactors. Nucl. Eng. Des. **33**, 178–195 (1975). https://doi.org/10.1016/0029-5493(75)90021-7
10. A. Marao, T. Kaliatka, E. Ušpuras, Analysis of processes in RBMK-1500 fuel assemblies during normal operation cycle. J. ENERGETIKA **56**, 8–18 (2010)
11. W.G. Luscher, K.J. Geelhood, Material Property Correlations: Comparisons between FRAPCON- 3.5, FRAPTRAN-1.5, and MATPRO. NUREG/CR-7024 Rev.1 PNNL-19417 Rev.1 (2014)
12. D. Gomes, A. Teixeira, Angra1 high burnup fuel behavior under reactivity initiated accident conditions. In: 2011 International Nuclear Atlantic Conference. Belo Horizonte, MG, Brazil, October 24–28 (2011)
13. C. Vitanza, U. Graziani, N.T. Fordestrommen, K.O. Vilpponen, Fission Gas Release from in-pile measurements. Report HPR-221.10, OECD Halden Reactor Project, (1978).
14. C. Vitanza, E. Kolstad, C. Graziani, *Fission gas release from UO2 pellet at high burnup, Topical Meeting on Light Water Reactor Fuel Performance* (American NuclearSociety, Portland, 1979)
15. Organisation for Economic Co-Operation and Development—Nuclear Energy Agency, Nuclear Fuel Safety Criteria Technical Review,64 p Paris (France) (2001)
16. H. Glaser, GRS Method for Uncertainty and Sensitivity Evaluation of Code Results and Applications. Sci.Tech. of Nucl. Installations, Vol. **2008**, Article ID 798901, p 7 (2008). https://doi.org/10.1155/2008/798901
17. M.Kloos, E.Hofer, SUSA Version 3.5. User's guide and tutorial. GRS, Garching, (2002)
18. K.J. Geelhood, W.G. Luscher, C.E. Beyer and al. Predictive bias and Sensitivity in NRC fuel performance codes. NUREG/CR-7001,PNNL-17644 (2009). NRC Job Code N6326
19. D. L. Hagrman, G. A. Reymann, MATPRO-version 11. A handbook of materials properties for use in the analysis of light water reactor fuel rod behaviour. Technical report, NUREG/CR-0497, TREE-1280 (1979)
20. IAEA-TECDOC-1496, Thermophysical properties database of materials for light water reactors and heavy water reactors. Final report of a coordinated research project (1999–2005)